

NGU Report 2000.012

**Interpretation of Low Latitude Magnetic  
Anomalies**

Report no.: 2000.012		ISSN 0800-3416	Grading: Open
Title: Interpretation of Low Latitude Magnetic Anomalies			
Authors: Les P. Beard, Berhe Goitom, and Jan Reidar Skilbrei		Client: NGU	
County:		Commune:	
Map-sheet name (M=1:250.000)		Map-sheet no. and -name (M=1:50.000)	
Deposit name and grid-reference: See summary below.		Number of pages: 31	Price (NOK): 180.-
Fieldwork carried out:		Date of report: 31.12.2000	Map enclosures:
Project no.:		Person responsible:	
2818.00		<i>Jan S. Rønning</i>	
Summary:  Magnetic data collected near the earth's magnetic equator is more difficult to interpret than high latitude magnetic data because the magnetic field intensity at the equator is smaller and because the ambient inducing field direction is horizontal. The low field strength produces correspondingly smaller anomalies, and the shallow field inclination produces several complications. Anomalies over magnetically susceptible bodies tend to be negative instead of positive, and the anomaly patterns may vary considerably with structural azimuth. Long north-south striking structures such as dikes and contacts can be magnetically invisible, except where the structures are broken or terminate. Equatorial anomalies tend to be stretched in an east-west direction. These latter two conditions can create the illusion of an east-west structural strike, regardless of the true geological strike. Synthetic modeling of magnetic fields produced by simple representations of geologically relevant structures such as ore bodies, pipes, dikes, folds, faults, and contacts help the interpreter to better understand the anomaly patterns present in real data. When magnetic remanence is dominant and the remanent field inclination is steep, it may have a strong affect on anomaly patterns. A shallow remanence inclination tends to rotate the induction-only anomaly pattern. Filters of various types—reduction-to-pole, vertical derivatives, analytic signal—can enhance interpretation of low latitude data, but all suffer limitations, especially when confronted with north-south striking structures.			
Keywords: Geophysics (Geofysikk)	Interpretation (Tolkning)	Magnetometry (Magnetometri)	
Anomaly (Anomali)	Airborne measurements (Flymåling)	Modelling (Modellforsøk)	
		Scientific report (Fagrapport)	

## CONTENTS

1	INTRODUCTION.....	4
2	CHARACTERISTICS OF LOW LATITUDE MAGNETIC ANOMALIES.....	4
3	INDUCED MAGNETIC ANOMALIES FROM SIMPLE STRUCTURES.....	5
4	REMANENCE.....	22
5	FILTERS.....	25
6	FIELD EXAMPLES—ETHIOPIA AND ERITREA.....	26
7	DISCUSSION AND CONCLUSIONS.....	28
8	ACKNOWLEDGMENTS.....	30
9	REFERENCES.....	30

## LIST OF FIGURES AND TABLES

- Fig. 1. Comparison of high- and low latitude anomalies.
- Fig. 2. Total field anomaly of a buried cube.
- Fig. 3. Total field anomaly of a vertical pipe.
- Fig. 4. Total field anomaly of a sill.
- Fig. 5. Total field anomaly of a ring dike.
- Fig. 6. Total field anomaly of a vertical fold belt.
- Fig. 7. Total field anomaly of a gravity fault.
- Fig. 8. Total field anomaly of a horizontally folded layer.
- Fig. 9. Total field anomaly of a 5000 m dike.
- Fig. 10. Total field anomaly of a 1000 m dike.
- Fig. 11. Total field anomaly of a dipping dike.
- Fig. 12. Remanence dominated anomaly of a buried cube.
- Fig. 13. Remanence dominated anomalies of dikes.
- Fig. 14. Aeromagnetic data—Ethiopia.
- Fig. 15. Aeromagnetic data--Eritrea

## **1 INTRODUCTION**

NGU project 2818.00—'Improved interpretation of low latitude magnetic anomalies'—was initiated in 1998 after NGU was involved with airborne geophysical surveys in Ethiopia and Eritrea flown by the Geological Survey of Finland in 1996. NGU was involved in the processing and interpretation of aeromagnetic and other data from both surveys. Although the processing of the aeromagnetic data was straightforward, interpretation of the magnetic data proved more challenging. In particular, the Ethiopia total field aeromagnetic map did not accurately reflect known major tectonic boundaries in the area. The Ethiopia survey area lay within a few degrees of the magnetic equator and the major contacts in the area trend north-south.

NGU's experiences with the Ethiopian and Eritrean surveys led to a project whose main goal was to obtain a better understanding of low latitude anomalies through synthetic modeling and through examination of low latitude magnetic data. At the close of the project, two presentations have been given at international conferences (Beard, 1999; Beard and Goitom, 2000), and one paper has been published in an international journal (Beard, 2000).

This report provides an introduction to the problems encountered in interpreting low latitude magnetic data, the low latitude magnetic anomalies produced by simple structures, and the effects of common filters on low latitude magnetic data.

## **2 CHARACTERISTICS OF LOW LATITUDE MAGNETIC ANOMALIES**

The earth's core-generated magnetic field approximates a magnetic field produced by a magnetic dipole. The poles of this field are roughly coincident with the earth's rotational axis, forcing the magnetic equator of the earth into approximate correspondence with the geographical equator. However, local deviations may be sizeable. For example, in western and central South America the magnetic equator lies between the geographical latitudes of 10°S and 15°S (Telford et al., 1993, Fig. 3.6B).

On the magnetic equator, the earth's dipolar field is oriented approximately north-south and is parallel to the earth's surface. Its magnitude is one-half that of the polar field. These characteristics combine to produce magnetic anomalies that are subtler and more complex than anomalies at high latitudes where the anomaly shape often mimics the geometry of the magnetic source rock. The horizontal inducing field at the equator causes the pattern of an induced magnetic anomaly to be highly dependent on its orientation. Long north-south oriented bodies may be almost invisible magnetically, even if the magnetic body has a high magnetic susceptibility. The same body oriented east-west may produce a large negative

anomaly. Finally, the lower intensity of the equatorial dipolar field implies smaller induced anomalies than would be produced at high latitudes by an identical body.

In order to get an idea of the effects of latitude on the shape of anomalies, we compare a magnetic map compiled over a portion of the Oslo Rift with what it might look like if it were located at the magnetic equator. Figure 1A shows the results of an NGU helicopter geophysical survey in which magnetic data were collected over an area of the Oslo Rift about 30 km north from Oslo (Beard, 1998). Ring dikes are prominent features, the result of magma emplacement following cauldron collapse (Thorpe and Brown, 1985). Other anomalies are related to compositional differences in igneous intrusions as well as fractures and faulting. The latitude of the survey area is at about 60°N. Figure 1B shows the same area as it might appear at the magnetic equator. We used a Geosoft (1986) reduce-to-equator (RTE) filter to transform the data to its equatorial pattern, then multiplied the data by 0.66 to mimic the anomaly magnitudes as they would occur at the equator. The RTE filter is stable, so the filtered result in Figure 1B is a fairly undistorted. All of the north-south trending anomalies in Figure 1A have disappeared nearly completely in Figure 1B, and the color bar in Figure 1B covers a much narrower range than in Figure 1A, indicating more muted anomalies. Also, the magnetic highs in Figure 1A have been transformed to lows in Figure 1B.

Low latitude anomalies can cause problems with some commonly used filter techniques. In particular, the reduction-to-pole (RTP) filter is unstable when applied to equatorial data, and can produce misleading artifacts.

In this report, we examine total field magnetic anomalies produced by simple bodies at or near the magnetic equator so that the reader may get a better feel for the kinds of anomaly patterns one can expect from commonly encountered geologic structures. We also explore the effects of remanent magnetization on low latitude anomalies and investigate the effects different filters have on anomalies.

### **3 INDUCED MAGNETIC ANOMALIES FROM SIMPLE STRUCTURES**

In this section total field anomalies produced at or near the magnetic equator are computed from models of simple structures. Only the induced component of the magnetic anomaly is modeled. Effects from remanent magnetization are considered negligible in these models. The models were chosen to represent simplifications of structures relevant to geological mapping or mineral exploration. The survey parameters were chosen as representative of an on-land airborne geophysical survey. In all the examples shown in this section, the magnetometer height is 100 m above ground level. Nevertheless, the anomaly patterns are scale-independent and could apply to any survey, however large or small. In all examples, the intensity of the ambient field at the magnetic equator (inclination 0°) is taken as 35000 nT and

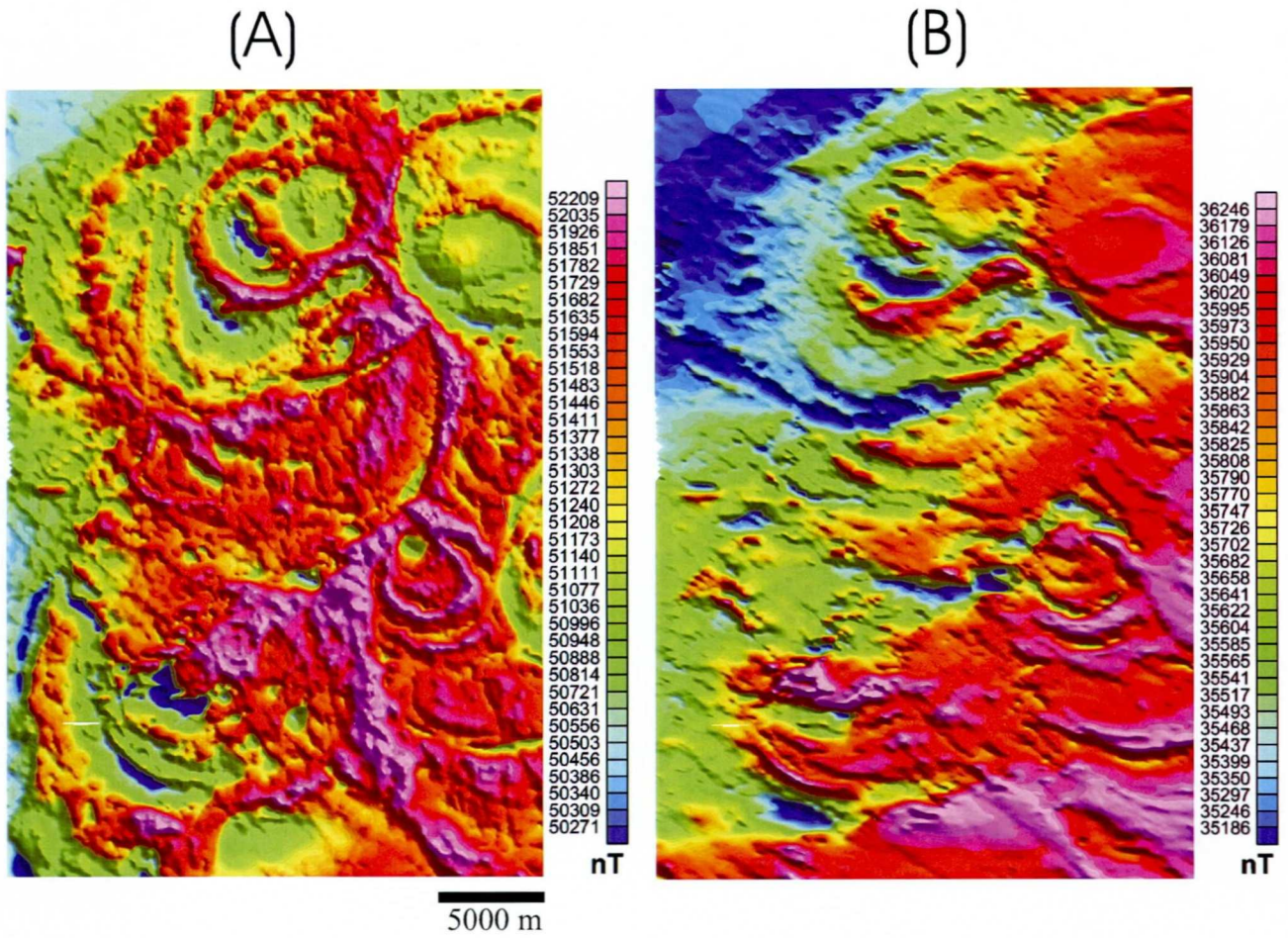


Fig. 1. Magnetic data from the Oslo Rift. (A) Map of measured data at about 60 degrees N latitude. (B) Map of same area as it would appear at the magnetic equator.

the magnetic declination  $0^\circ$ . In examples where anomalies were computed for a magnetic inclination of  $15^\circ\text{N}$ , an ambient field of 40830 nT was used. All color plan view figures are illuminated at an angle of  $45^\circ$  above the horizon from the northeast. In all examples, north is toward the top of the figure.

### **3.1 Laterally equidimensional bodies**

Laterally equidimensional bodies form an important class of geologically relevant structures. Sulfide ore bodies may possess a roughly equidimensional character. Kimberlite pipes, a major target in diamond exploration, often have an equidimensional surface expression. Sills and ring dikes may also show rough lateral equidimensionality. Laterally equidimensional structures show almost the same anomaly regardless of orientation, making the job of interpretation somewhat easier than with structures having a strike direction.

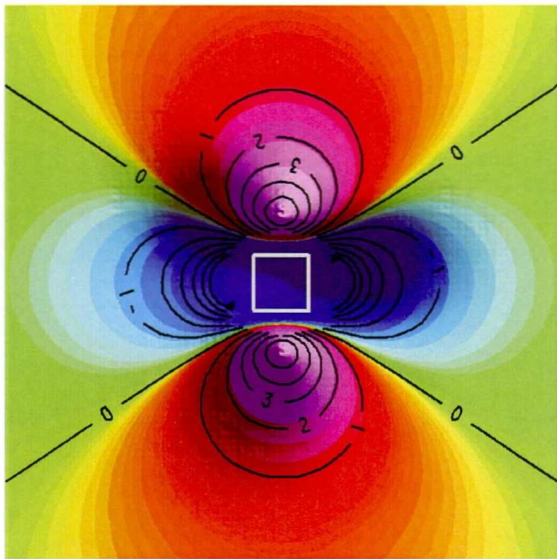
#### **3.1.1 Compact body**

Ore deposits may vary greatly in geometry, but many acquire a compact, roughly equidimensional form that can be modeled as a cube. Although the magnetic characteristics of ore deposits also vary considerably, many have significant concentrations of magnetic minerals associated with them that can produce sizeable magnetic anomalies. For example, consider a cubic ore body 400 m on edge and buried 100 m below the earth's surface and having a magnetic susceptibility of 0.01 SI. An ore body of this size would interest most mining companies. What kind of magnetic signature is produced by such a body at low latitudes? Figures 2A and 2B show the magnetic anomaly patterns that would be expected at the magnetic equator and at  $15^\circ$  magnetic north latitude, respectively. In both cases, the dominant feature is the negative anomaly over the body. To the north and south of the body are smaller positive anomalies. Figure 2C shows north-south survey altitude profiles over the center of the body. The magnitude of the negative anomaly is between 20 and 25 nT. At  $15^\circ\text{N}$ , the anomaly is larger because the inducing field is larger—40830 nT compared to the 35000 nT equatorial field—and the positive lobes are asymmetric. At Norwegian latitudes, this same body would produce a positive anomaly over the body up to 4 times larger than the magnitude of the equatorial negative anomaly. Regarding the negative anomaly over the body, another feature to note is how wide the anomaly appears along an east-west profile. This is characteristic of low latitude magnetic anomalies and is a common source of interpretational error.

#### **3.1.2 Vertical pipe**

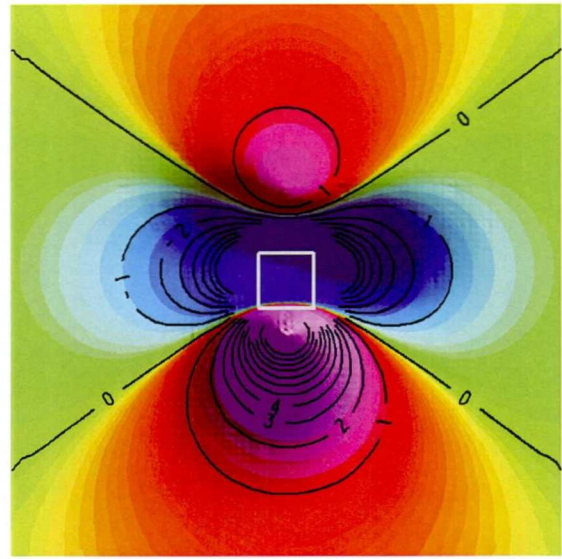
Kimberlite and lamproite pipes (diatremes) are common source rocks for diamonds. The diameter of these pipes can be small (100 m) and therefore make difficult targets in airborne

(A)



400 m

(B)



(C)

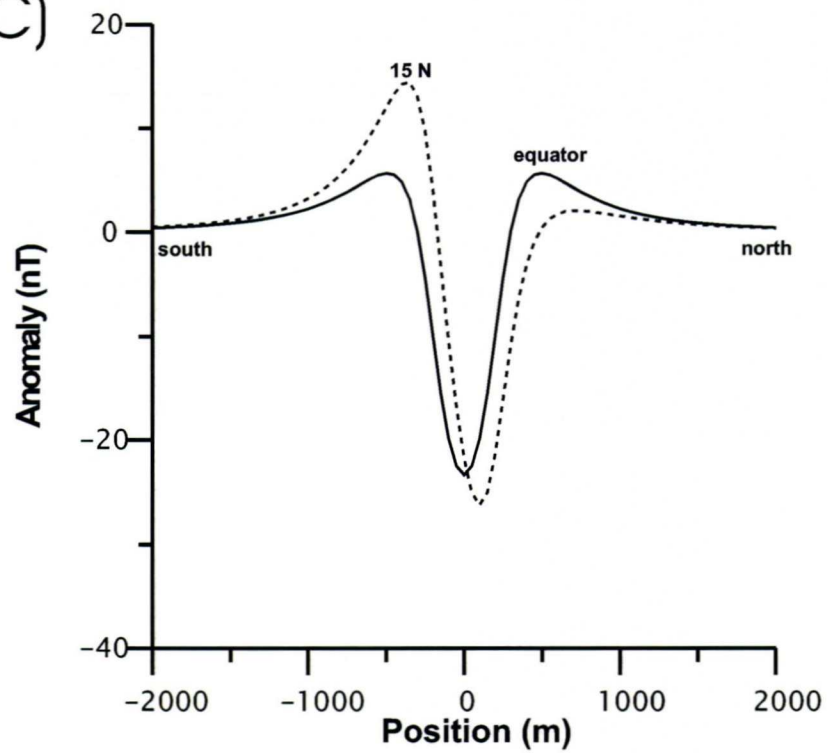


Fig. 2. Magnetic anomalies produced by cubic bodies (A) at the magnetic equator and (B) at 15 deg N magnetic latitude. Part (C) shows N-S profiles over the center of each cube.



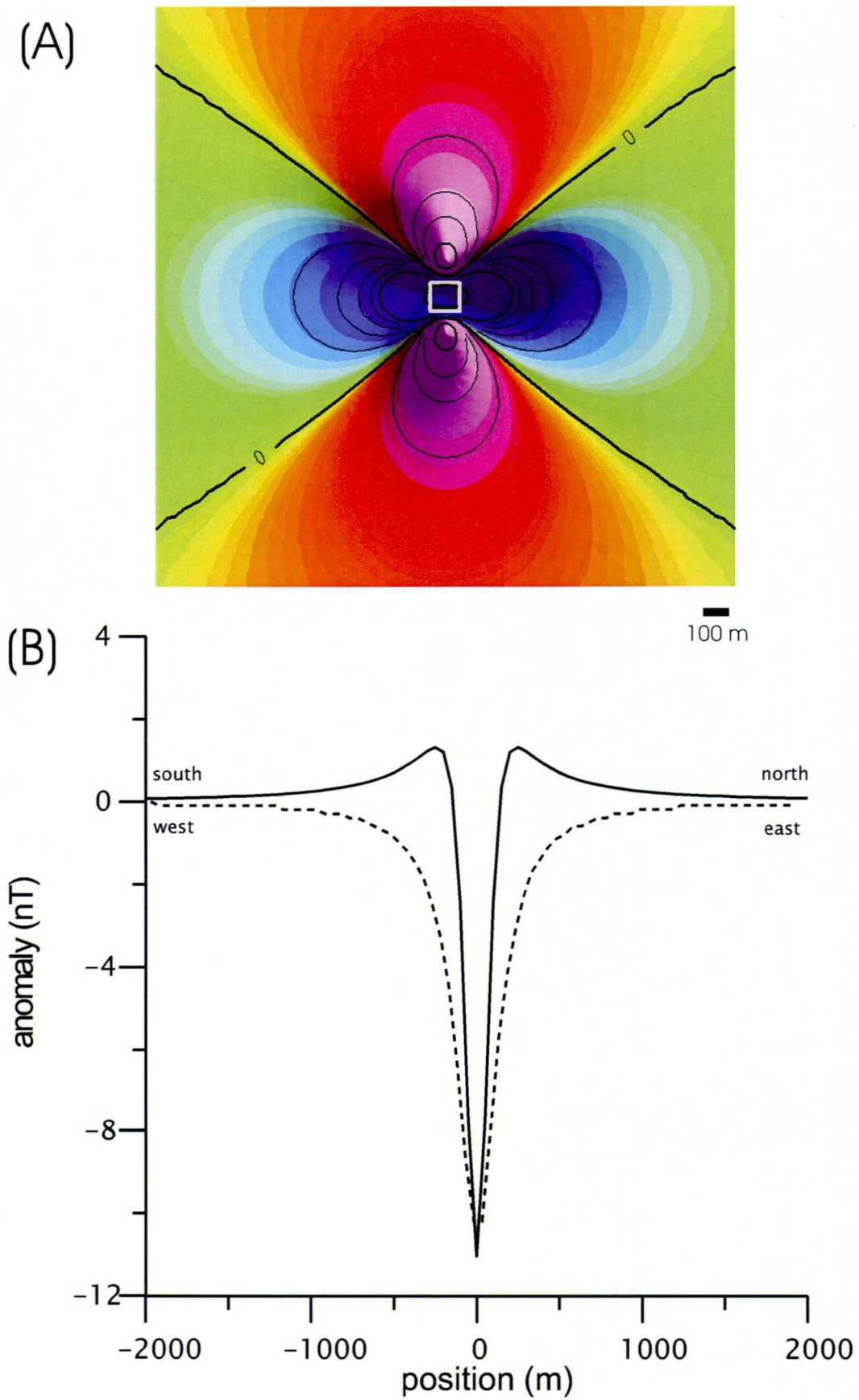


Fig. 3. Total magnetic field anomaly over a vertical pipe-like structure. (A) Plan view of anomaly. (B) North-south (solid curve) and east-west (dashed curve) profiles over the center of the vertical pipe.

exploration. However, many pipes contain significant magnetic mineralization and so produce detectable magnetic anomalies if the sensor passes nearby. As might be expected, a vertical pipe at the magnetic equator produces an anomaly similar to that of a compact equidimensional body, i.e. a modestly large central negative anomaly over the pipe with small positives flanking the body to the north and south. Figure 3A shows the plan view equatorial anomaly of a vertical pipe with a 100 m x 100 m outcrop. The magnetic susceptibility of the body is 0.01 SI, a value associated with an Australian lamproite pipe (Drew and Cowan, 1994). Shown in Figure 3B are profiles over the center of the body at sensor altitude (100 m above ground level). The maximum magnitude of the central negative anomaly is about 11 nT.

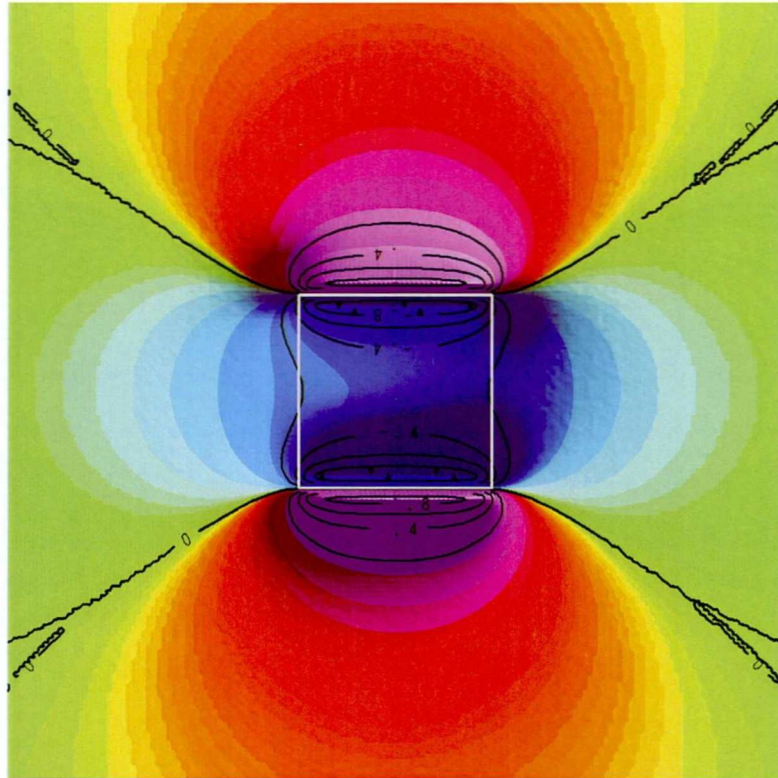
### **3.1.3 Sill**

In layered sedimentary units, lava may intrude the layers creating extensive but relatively thin tabular units known as sills. Sills are difficult targets at low latitudes because the magnetic anomaly is most pronounced at the edge of the sill, and thin sills having a gabbroic composition may produce low latitude anomalies at the edges of only a few nanoteslas. If the edges are irregular, even these small anomalies may be lost in background geological noise. Shown in Figures 4A and 4B are sensor height anomaly patterns produced at the magnetic equator and at 15° N magnetic latitude, respectively, by a 2000 m x 2000 m wide sill that has a thickness of 2 m and a magnetic susceptibility of 0.02 SI (a middle range value for gabbro or basalt according to Clark (1994)) and is buried 20 m deep. The maximum peak-to-trough anomalies are less than 2.0 nT in both cases. The main difference between the two cases is that at 15° N, the east and west edges of the sill exhibit more pronounced lows than do the equatorial sill, and these may be enhanced by edge-detection filters.

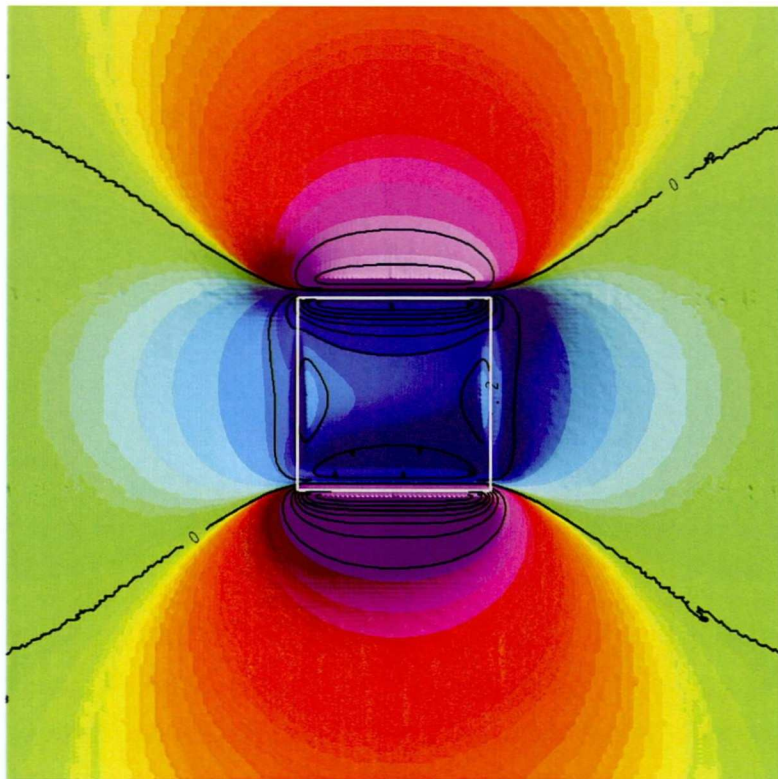
### **3.1.4 Ring dike**

Ring dikes are circular or arcuate igneous intrusions that form when a central block subsides in a tensional stress field (Thorpe and Brown, 1985). The walls of the ring dike are up to several hundred meters thick and near-vertical. The bulk of the ring dike, combined with the absence of any extended north-south trending features, make it a promising feature for detection even at equatorial latitudes. Shown in Figure 5 is the total field magnetic anomaly produced by an outcropping ring dike having walls that are 200 m thick and an outer diameter of 2814 m. Its depth extent is 4000 m. The susceptibility of the ring is 0.02 SI. In this example, the magnetic latitude is 0°. The ring is clearly evident as a nearly circular magnetic low overlying the ring. The anomalies on the north and south sides of the ring are about -150 nT, whereas the east and west side anomalies are only -50 nT. The small central positive anomaly rises to about 15 nT. These magnitudes are high at low latitudes, making the ring dike one of the more easily identified structures in a low latitude aeromagnetic survey.

(A)



(B)



2000 m

Fig. 4. Magnetic anomalies from a 2000 m x 2000 m x 2 m horizontal sill: (A) anomaly at magnetic equator, (B) anomaly at 15 deg magnetic north.

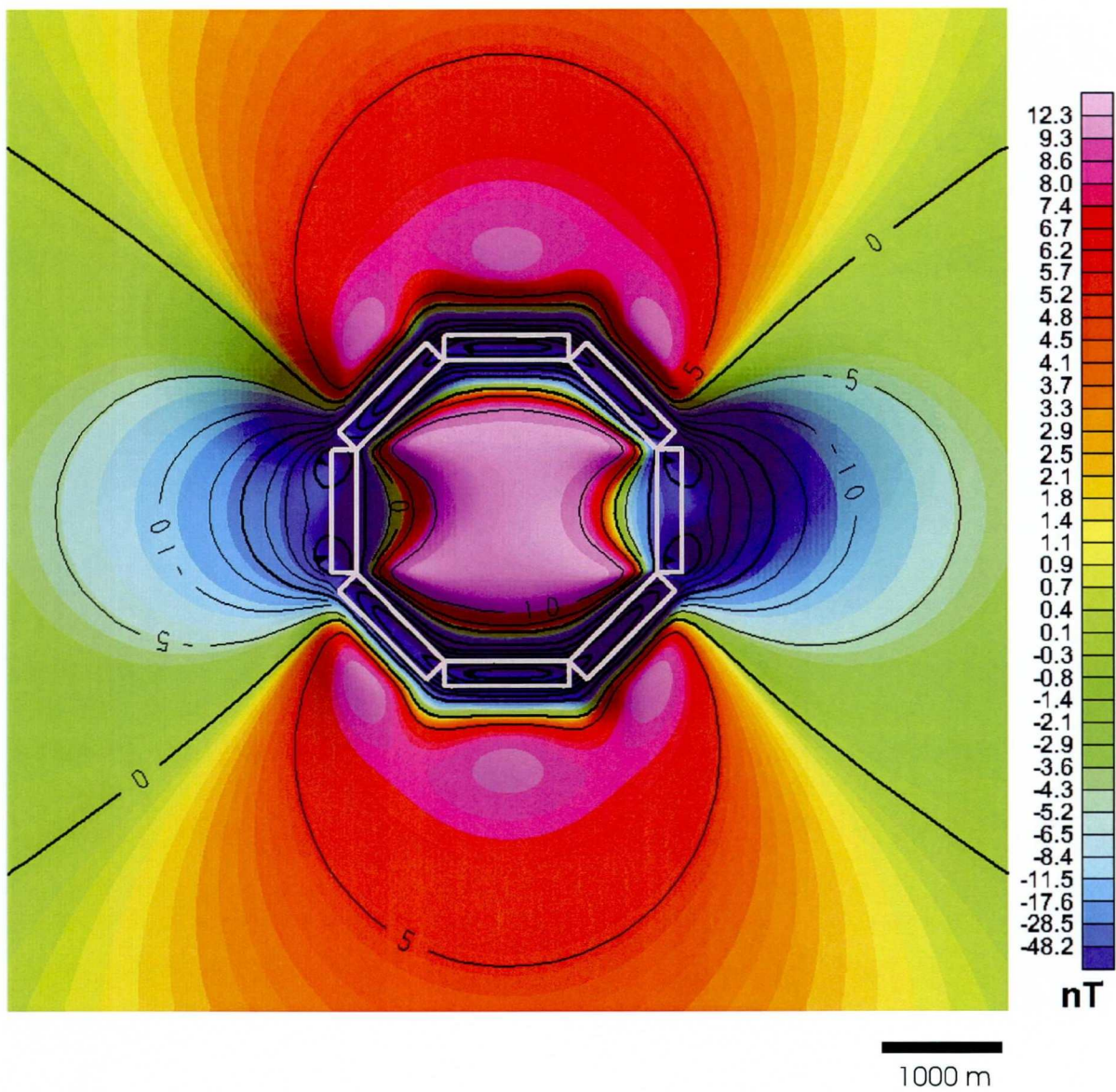


Fig. 5. Total field anomaly of a ring dike at the magnetic equator. The outer diameter of the ring is 2814 m. The inner diameter is 2414 m.

## **3.2 Laterally extended bodies**

Laterally extended bodies include structures such as folds, faults, horst-and-graben features, and dikes. At low latitudes, the magnetic anomaly pattern from such bodies exhibits a high degree of azimuthal dependence. When the strike of a laterally extended body is north-south, it may be almost invisible magnetically, whereas an east-west strike may show a strong negative anomaly over the body. Shown below are examples of low latitude anomalies from idealized laterally extended bodies.

### **3.2.1 Vertical folds and horst-and-grabens**

Figures 6A and 6B show anomalies that result from a series of symmetric vertical folds at the magnetic equator. The folds have a wavelength of 600 m and an amplitude of 300 m as measured from crest to trough (commonly called the peak-to-peak, or P-P, amplitude). The peaks of the folds outcrop at the earth's surface and the thickness of the layer is 500 m. The susceptibility of the layer is 0.01 SI. Irrespective of these parameters, if the fold belt strike were in the direction of the ambient field declination, usually nearly north-south, no anomaly would be produced. The fold belt would be magnetically invisible for any geologically reasonable magnetic susceptibility contrast. However, if the strike of the fold belt is several degrees off the ambient field declination, the fold pattern begins to appear as alternating high and low lineaments. The magnetic highs occur over the troughs of the folds and the magnetic lows over the outcropping crests. In Figure 6A, the strike angle is 20° east of north. The P-P magnitude is about 10 nT, a value high enough to stand out above most background magnetic variation. However, the thickness of the magnetic layer is 500 m. A layer only 50 m thick would produce only a 4.5 nT anomaly. Figure 6B shows the anomaly pattern for an east-west striking fold belt. The P-P amplitude in this case is almost 50 nT. Thus, even fairly thin folded layers may be delineated if they strike nearly east-west.

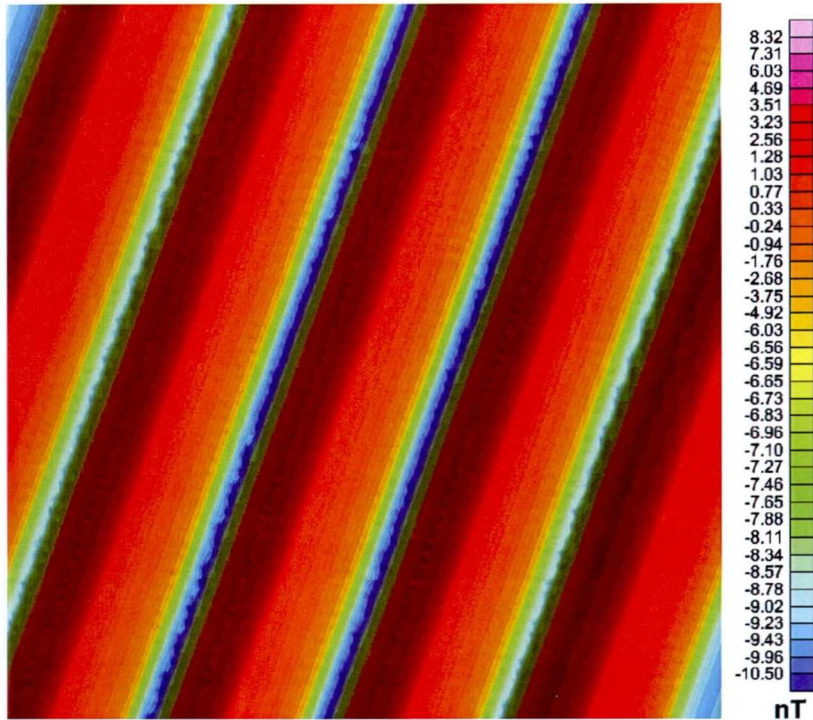
Horst-and-graben structures would produce anomalies similar to a vertical fold belt.

### **3.2.2 Gravity faults and contacts**

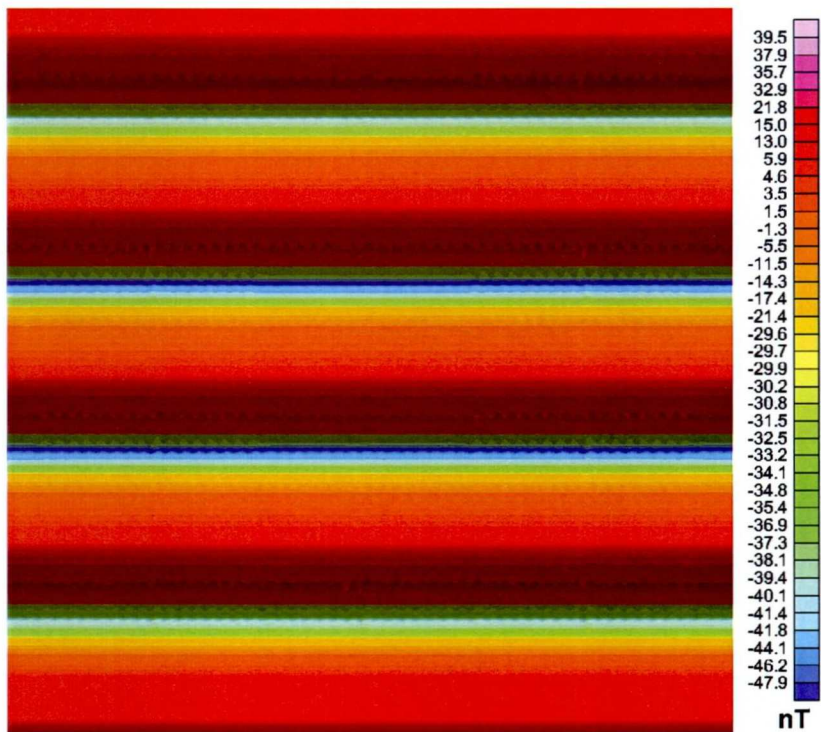
Gravity faults occur under tensional stress regimes and may occur in a wide variety of scales. Localized slump blocks may have vertical offsets of a few meters whereas offsets in rift valleys may be hundreds of meters. As with any extended two-dimensional structure at the magnetic equator, a north-south strike will produce no magnetic anomaly, whereas a strike direction several degrees off the north-south axis can yield a detectable anomaly.

Although the angle of the fault will influence the width of the anomaly, all will have the same basic shape, and for illustrative purposes we use a vertical fault model. Our model represents a 1000 m thick basaltic unit having magnetic susceptibility of 0.01 SI. The unit is faulted and

(A)



(B)



500 m

Fig. 6. Magnetic anomaly patterns produced by vertical folding with the structural strike at an azimuth of (A) 20 degrees east of north and (B) east-west. Note the difference in magnitudes of the scale bars. The magnetic lows correspond to peaks in the folding of the magnetic layer. Wavelength of folding is 600 m.

has a vertical offset of 200 m. The fault angle is  $30^\circ$  east of north, and the downthrown block is on the northwest side of the fault. The upthrown portion of the fault block outcrops at the earth's surface. Figure 7A shows the plan view equatorial anomaly produced by the fault model shown in Figure 7C. The maximum P-P anomaly at the fault is about 24 nT, as can be seen in the profile in Figure 7B. Note that the profile pattern is opposite what one would expect from the same structure at high latitudes. The positive part of the anomaly is on the downthrown side. Were the strike of the fault east-west, the pattern would be similar, but the P-P anomaly would increase to 178 nT. If one of the fault blocks rotated so that the fault was dipping, one would expect the pattern to show an increased anomaly along strike in the direction of increasing depth to the fault line.

Geological contacts would produce anomalies similar to a vertical fault.

### **3.2.3 Horizontal folds**

Horizontal folds are capable of producing a complicated but distinctive anomaly pattern, even if the general strike of the fold belt is north-south. Figures 8A and 8B show equatorial total field anomaly patterns produced by a fold belt trending north-south and northeast-southwest, respectively. The fold thickness is 300 m. The wavelength of folding is 1800 m with a peak-to-peak fold amplitude of 900 m. The depth extent of the folded layer is 1000 m. The magnetic susceptibility of the folded layer is 0.01 SI. Because the horizontal folds put the magnetic layer at an angle to a north-south axis, even when the dominant trend of the fold belt is north-south, as in Figure 8A, a significant anomaly may be produced. In this case, the P-P anomaly is 35 nT and the negative maximum  $-23$  nT, values easily detectable above most background variation. When the folded layer strikes northeast-southwest, the negative maximum over the folded layer increases to  $-78$  nT, producing a P-P anomaly of 90 nT. In both cases the dominant feature is the magnetic low over the folded layer. Smaller, but still significant, positive anomalies occur at the peak and crest of the folds.

### **3.2.4 Dikes**

Dikes should be placed in a slightly different category than the other structures discussed in this section because they tend to be more limited in length. Whereas a typical airborne survey might fail to completely encompass a major contact or fold belt, dikes are more likely to have one or both terminations inside the survey area. This has important ramifications with respect to detection, particularly if the strike of the dike is north-south. Beard (2000) conducted a model study of north-south trending equatorial dikes and demonstrated that a dike's most significant anomalies are produced at its end points.

Shown in Figures 9 A-C are total field responses at different azimuths from a 5000 m long vertical dike having a width of 20 m and a depth extent of 500 m. The magnetic susceptibility

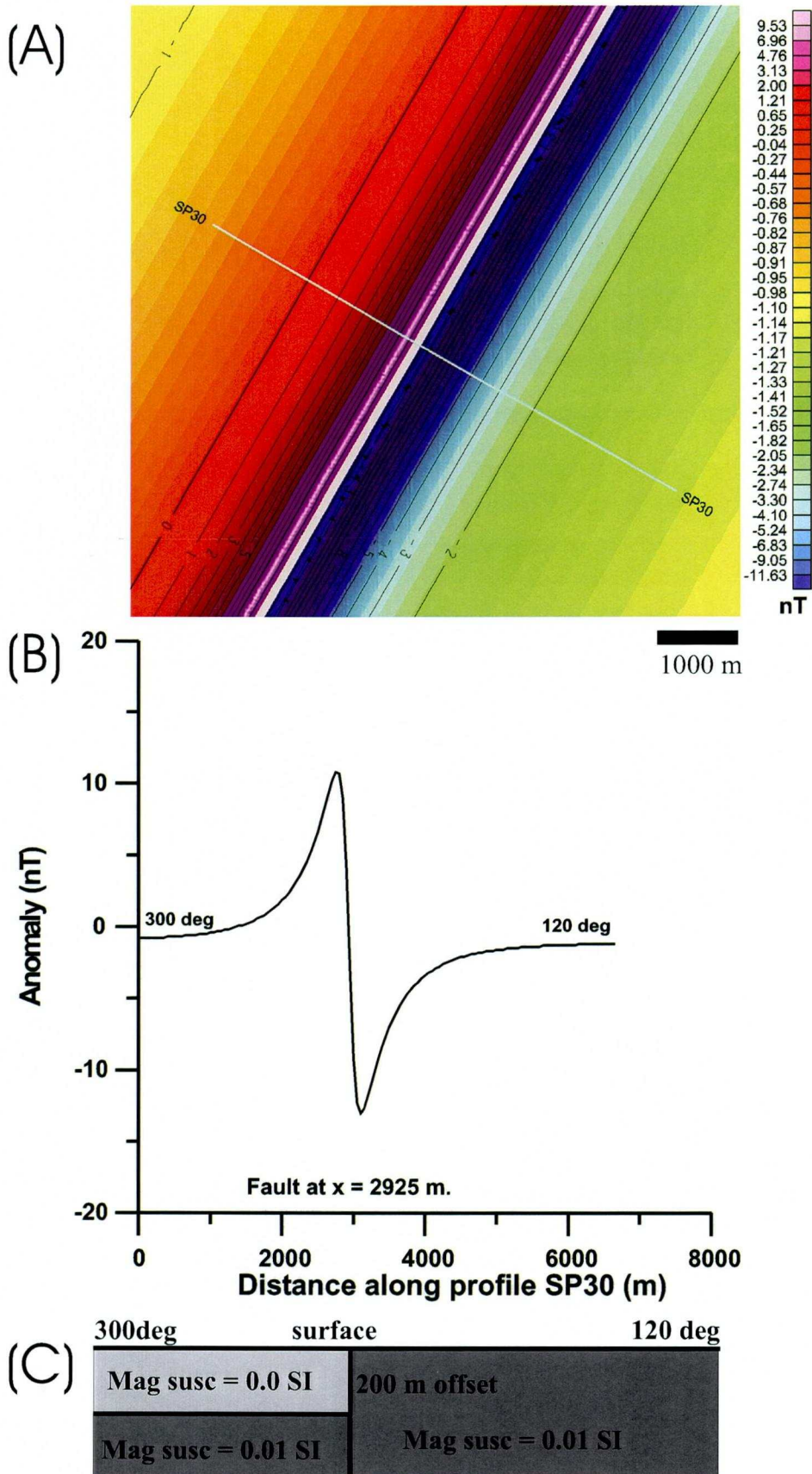


Fig. 7. Total field magnetic anomaly produced by a vertical fault at the magnetic equator. Fault block offset is 100 m. Fault strike is 30 degrees east of north. The downthrown side is on the northwest side of the fault (grey line). (A) Plan view of anomaly. (B) Profile denoted 'SP30' across the fault. (C) Cross-section with fault location matching location in part (B).



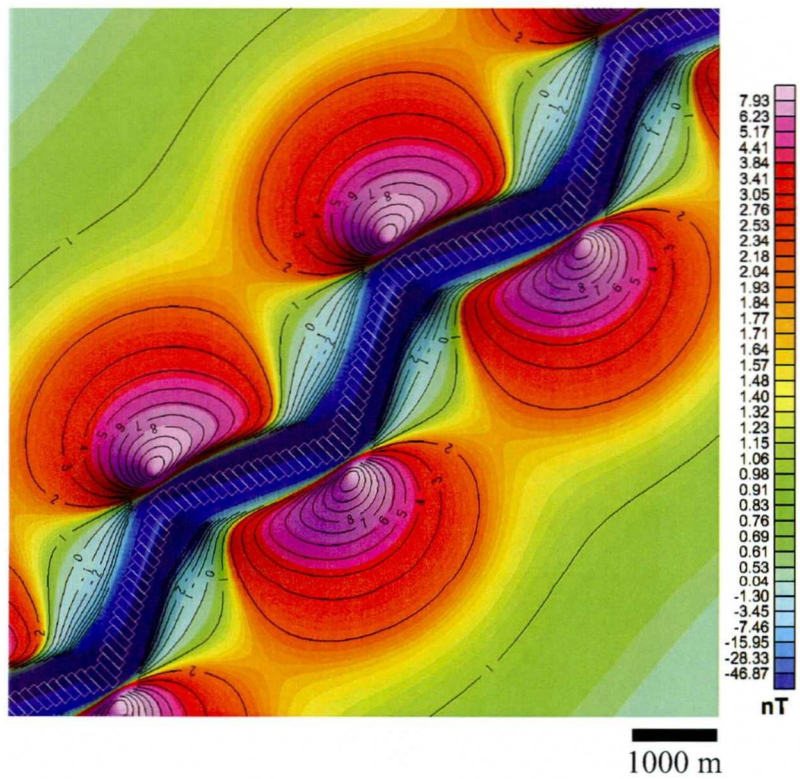
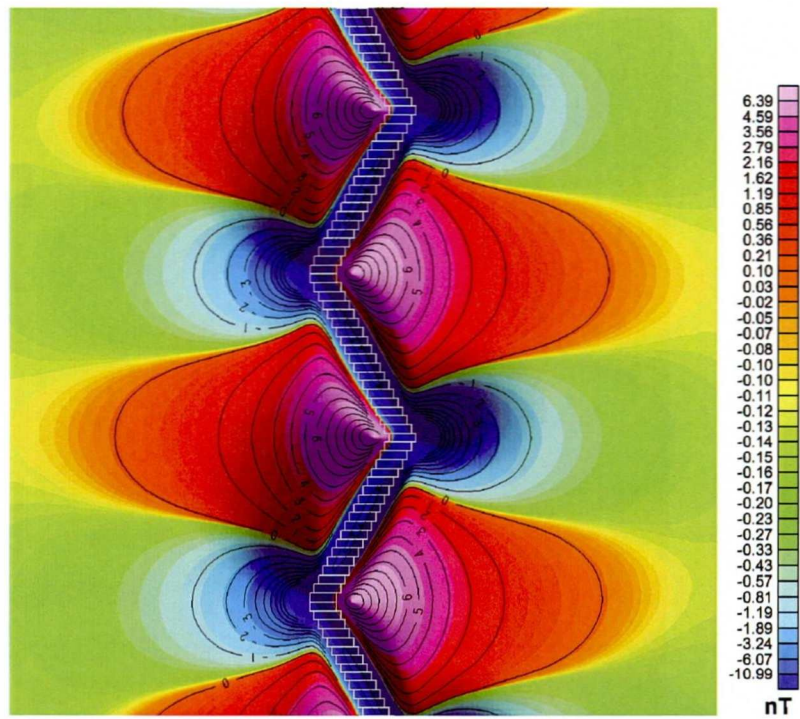


Fig. 8. Total field anomalies produced by a horizontally folded layer at the magnetic equator. (A) General strike: N-S. (B) General strike: NE-SW.

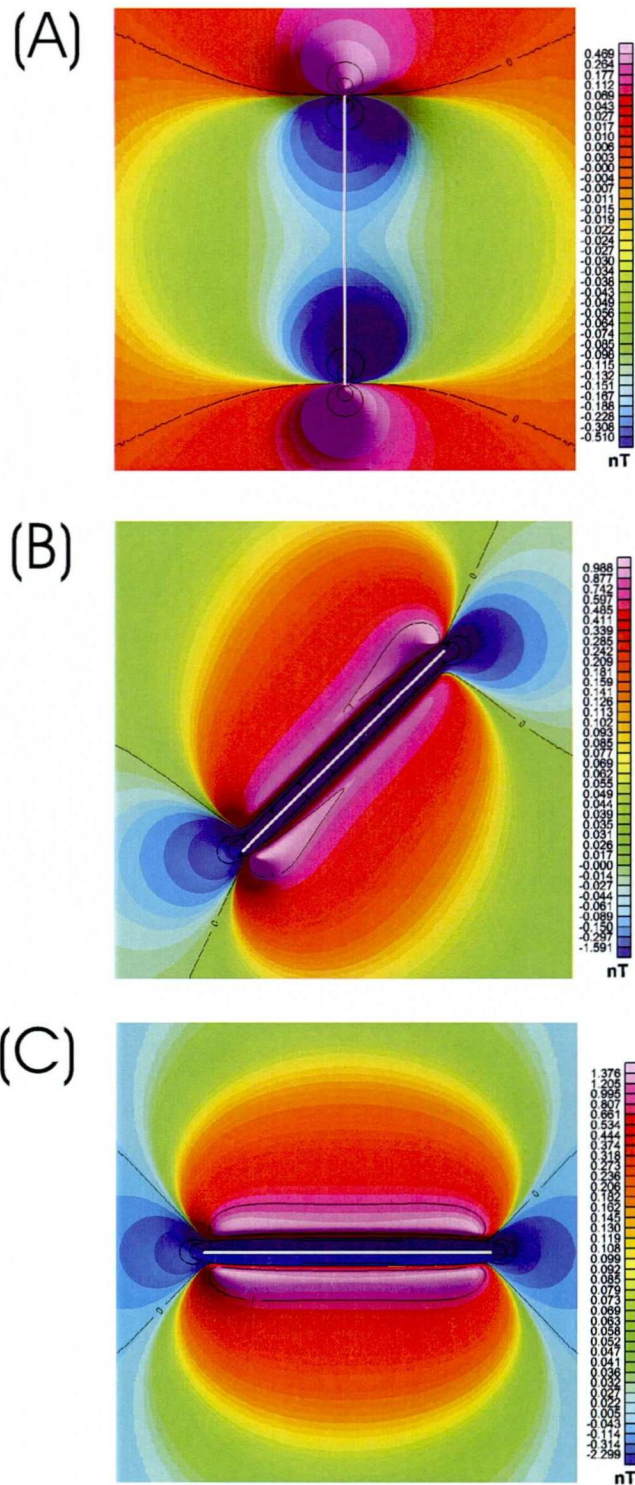


Fig. 9. Magnetic anomalies produced by a dike at the magnetic equator. The dike is 5000 m long, 20 m wide, and 500 m in depth extent. It outcrops at the surface. The magnetic susceptibility of the dike is 0.02 SI. (A) N-S strike. (B) 45 degree strike. (C) E-W strike.

of the dike is 0.02 SI. As can be seen in Figure 9A, the main body of a north-south oriented dike at the magnetic equator is almost invisible magnetically, but the dike's presence may be inferred from the distinctive anomalies at its north and south terminations. Even so, the P-P magnitude of the termination anomalies are only about 6 nT. Figure 9B shows the anomaly produced by the same dike with an azimuth  $45^\circ$  from north. The maximum P-P anomaly is now about 15 nT. The dominant feature is a magnetic low over the main portion of the dike. This feature is also dominant in an east-west striking dike (Figure 9C), but in this case the P-P amplitude has increased to 20 nT. Although these anomaly magnitudes appear large enough for detection, they in fact occur over quite small areas, and could be easily missed in an airborne survey having flight line spacing of over 100m. However, a wider dike, or one with higher susceptibility, would have a correspondingly larger anomaly, making it more easily detectable from the air.

Figure 10A shows the equatorial magnetic anomaly produced by a similar dike in a north-south orientation, but one having a 1000 m strike length instead of 5000 m. In this case the anomaly resembles that of the cubic structure in Figure 2 because the negative lobes of the termination anomalies are close enough together that they begin to overlap. However, they can be distinguished because the negative portion of a compact body anomaly is usually much larger than its positive lobes whereas with a dike they positive and negative portions are almost equal. Compare the anomaly shape of Figure 10A with the anomaly produced by north-south oriented steel pipes. Three steel pipes placed side-by-side produced the anomaly. Each pipe is 6 cm wide and 6 m long. The data were collected in Asmara, Eritrea, a city having a magnetic latitude (inclination) of about  $16^\circ\text{N}$  and a declination of  $2^\circ\text{E}$ . Although the magnetic susceptibility of the pipe is not known, measurements by Ravat (1996) and Eskola et al. (1999) indicate high susceptibilities (100 SI or more) for unrusted steel. From the shape of the anomaly magnetic induction appears to dominate any remanence effects.

Anomalies of the type shown in Figure 11 occur fairly commonly in low latitude data sets. Such anomalies have two roughly equal lobes of opposite polarity. A dipping north-south trending dike will cause such an anomaly if induction is dominant. If the structure dips toward the north, the south part of the anomaly will be positive. A southward dip will cause the positive lobe to be on the north side. This type of anomaly can easily be mistaken for a 3-D body. In Figure 11 the dike is exactly the same as the dike described in Figure 9A, but it has a  $26.6^\circ$  dip toward the north. Although the south termination of the dike outcrops and produces a modest anomaly, the north termination is too deeply buried to produce a significant anomaly. In this example the positive lobe at the southern termination has a magnitude of 1.5 nT and the negative lobe is slightly larger at  $-4.3$  nT.

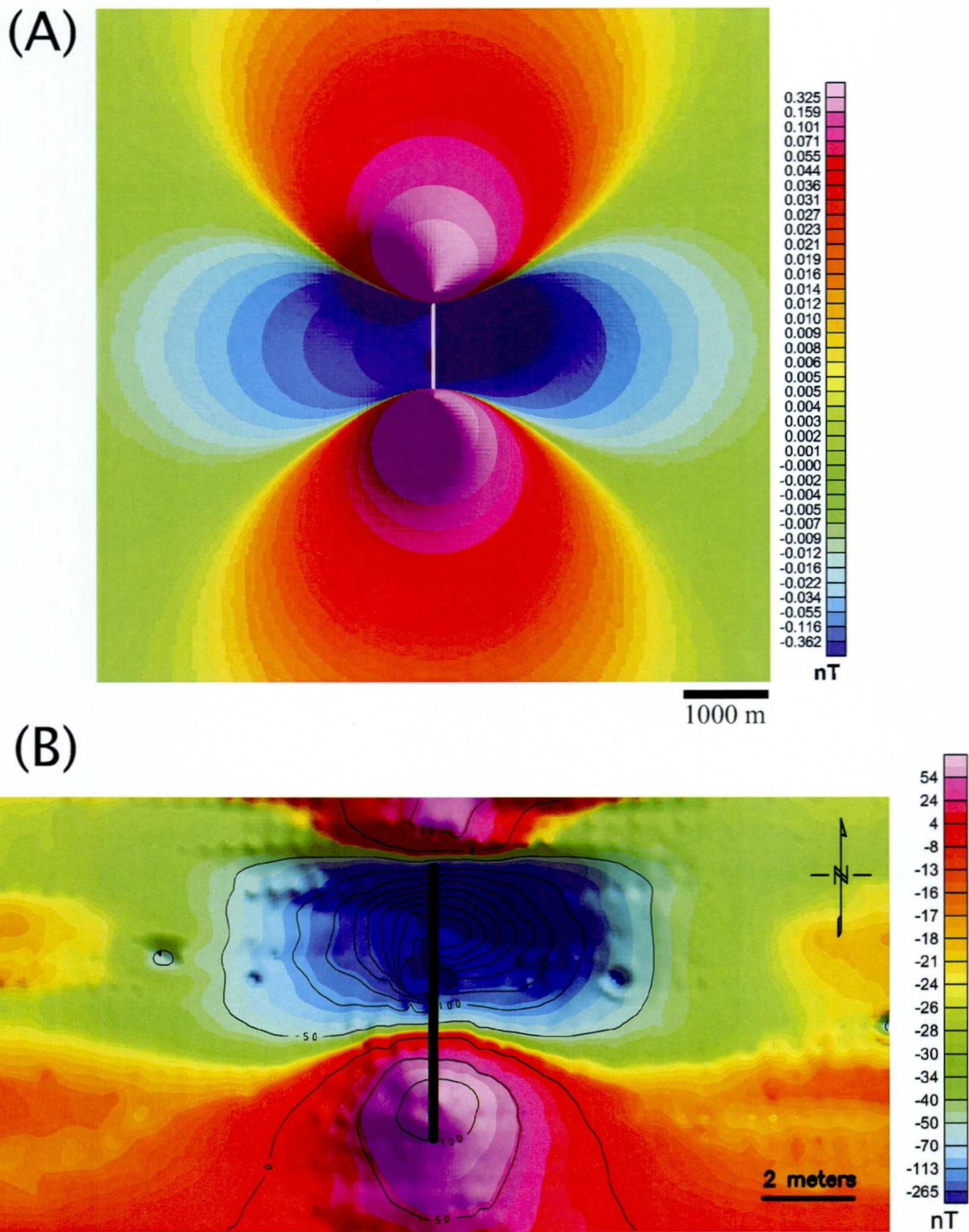


Fig. 10. (A) Magnetic anomaly at the magnetic equator of a dike having the same parameters as in Figure 9A, except that the length is 1000 m. (B) Anomaly produced by N-S oriented steel pipes, Asmara, Eritrea.

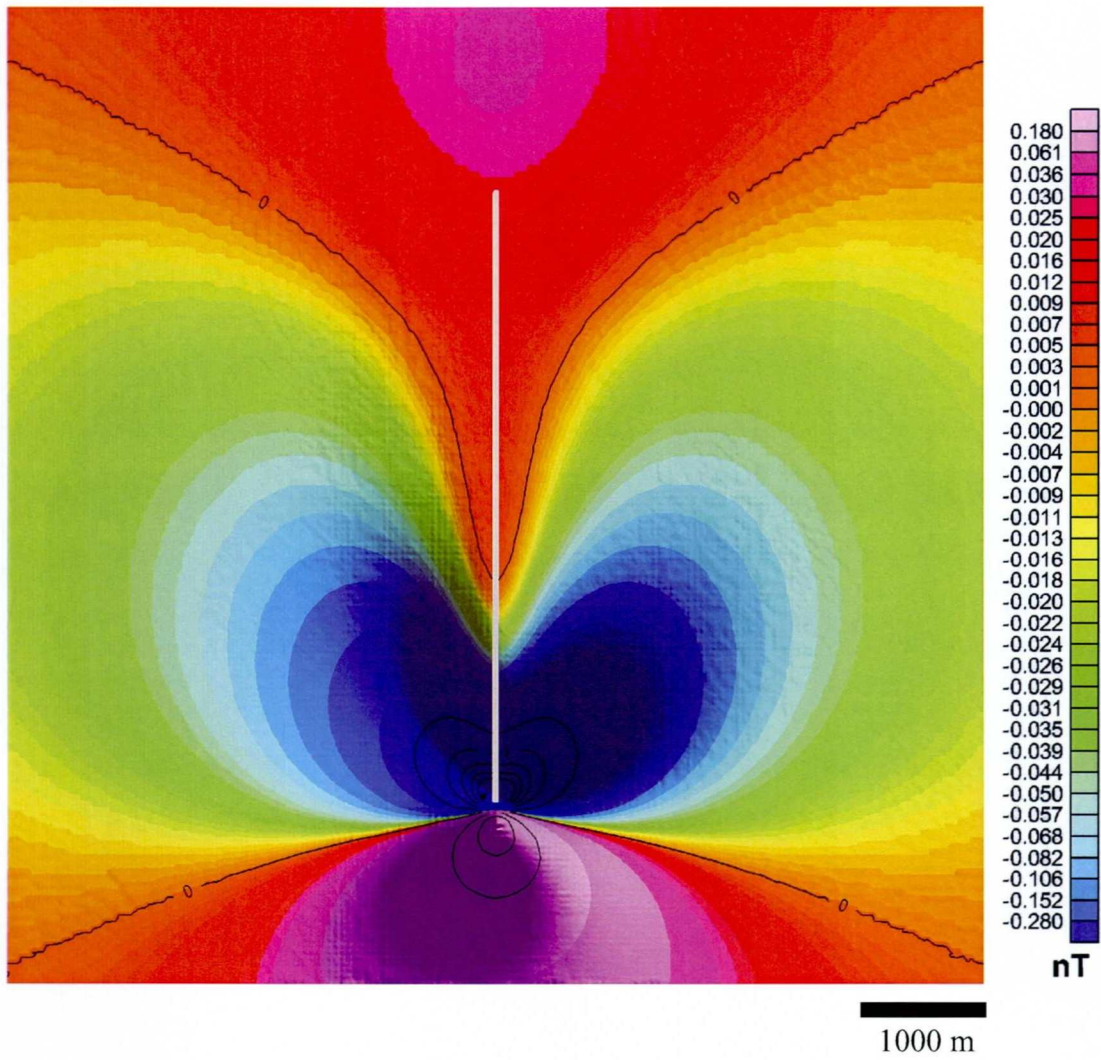


Fig. 11. Total field anomaly of a dike dipping at an angle of 30 degrees to the north. The dike is exactly the same as in Fig. 9, except for the dip angle.

## 4 REMANENCE

In all of the examples of section 3 the anomalies shown were produced by magnetization induced by the earth's ambient field. Induced magnetization falls to zero in a field-free environment. However, many rocks contain a more or less permanent magnetization—remanent magnetization—that is independent of the ambient field. The total magnetic field is a sum of the induced and the remanent magnetization. The ratio of remanent magnetization to induced magnetization is called the Koenigsberger ratio, or more simply the Q-value. A Q less than unity implies induction is dominant whereas a Q greater than unity implies remanent magnetization dominates. Following the usual formulation (Blakely, ch. 5, p.90, 1995), if the ambient magnetic field has a magnitude of 35000 nT, then the remanent magnetization is given by

$$M_{rem} = 27.852 \cdot Q \cdot \chi \text{ A/m}$$

where  $\chi$  is the unitless SI measure of magnetic susceptibility. Remanent anomalies appear in a wide range of environments, but are particularly common in basaltic rocks, porphyry ore bodies, banded iron formations, and skarns. Remanence may complicate the interpretation of a magnetic anomaly, but may also enhance the detectability of a body by increasing the magnitude of the anomaly. This can be particularly important at equatorial latitudes where induction anomalies are small. In this section we do not attempt a comprehensive study of remanent anomalies, but rather examine a small subset of the bodies modeled in the previous section in the hope that a few examples can illustrate the importance of identifying remanence when it occurs in low latitude field data. The anomalies that can be produced by combinations of remanent and induced magnetization are so varied that an analysis of field data will certainly require careful computer modeling.

### 4.1 Equidimensional bodies

Shown in Figure 12A is an anomaly pattern commonly seen at low latitudes, an anomaly with two roughly equal positive and negative lobes aligned north-south. As mentioned in section 3.2.4 and illustrated in Figure 11, a dipping, north-south striking dike can produce such an anomaly. However, an equidimensional body possessing remanent magnetization may produce a similar anomaly if the direction of remanent magnetization is appropriately aligned. The anomaly in Figure 12A is produced by a cubic body having the same dimensions and physical parameters as the cubic body described in section 3.1.1. The only difference is that the body has a Q of 2, that is, remanence dominates induction by a factor of 2. In most orientations of the remanent field, the remanence anomaly superposes with the induction anomaly so as to produce an anomaly that looks like a rotated version of Figure 2a, but if the remanence direction is steeply inclined and has a declination opposite the normal field, an anomaly similar to that of a dipping dike is produced. In Figure 12a, the remanent inclination is 70° and the declination is 180°, opposite the inducing field. A south-to-north profile

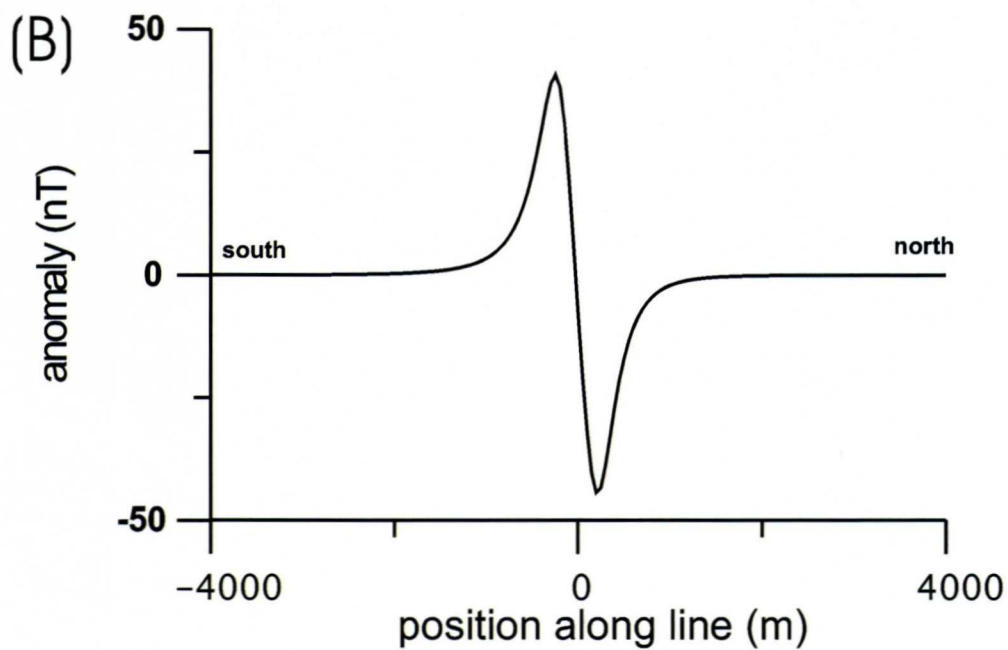
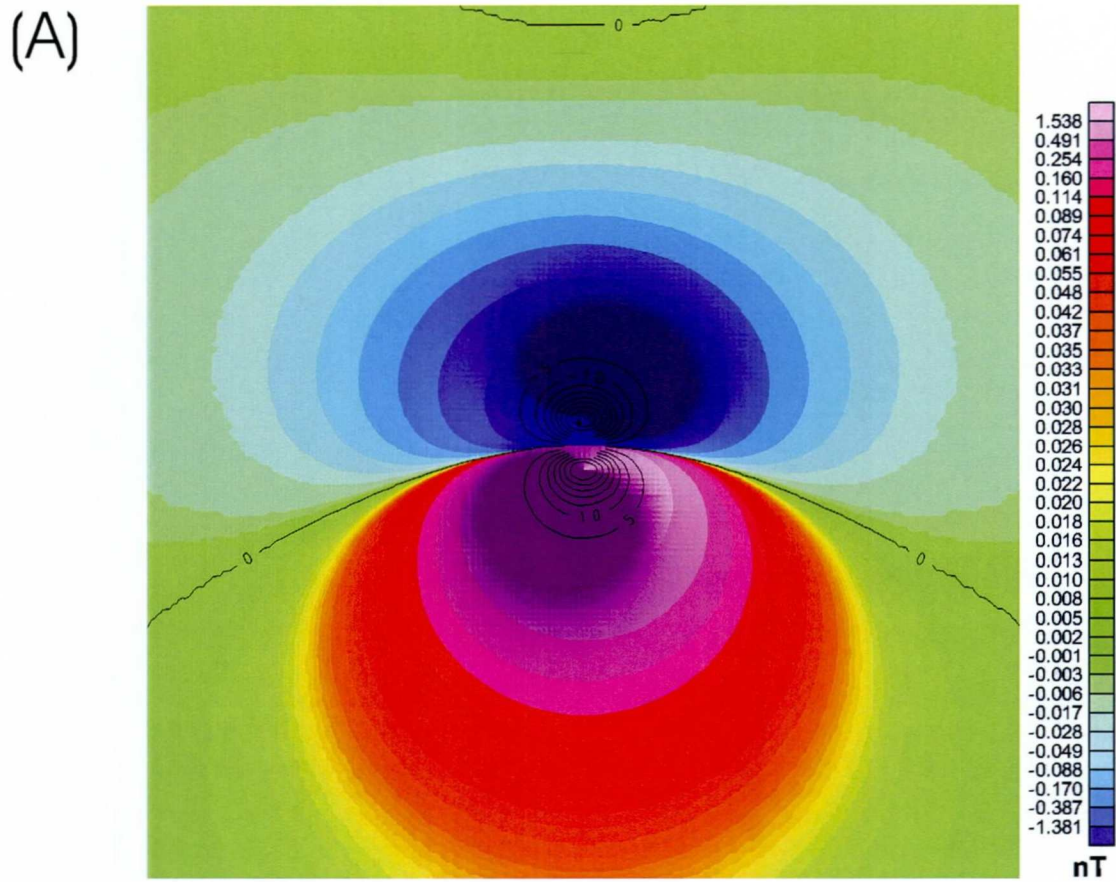
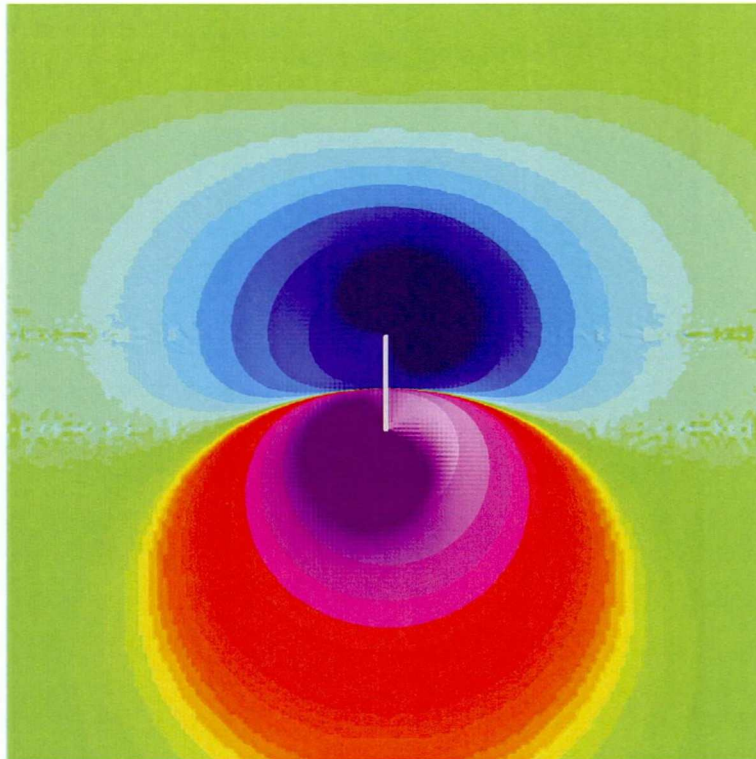
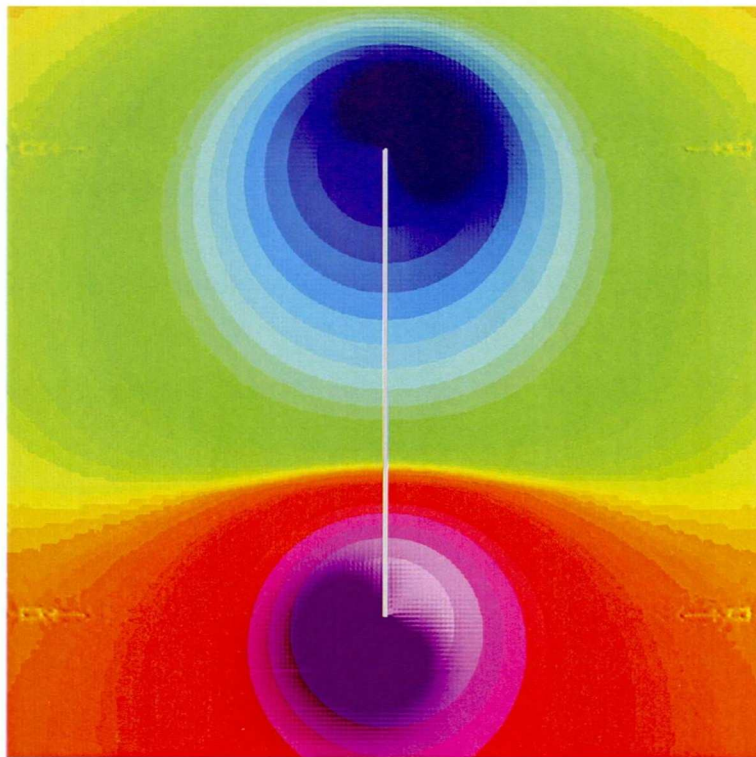


Fig. 12. Effect of remanent magnetization on an equidimensional body. The magnetic source is the same as in Fig. 2, but with  $Q=2$ . (A) Magnetic anomaly in plan view. (B) South-to-north profile over the center of the body.

(A)



(B)



1000 m

Fig. 13. Remanence dominated anomalies from vertical dike.  $Q = 2$ , remanence inclination = 70 deg, remanence declination = 180 deg. All other parameters same as for dike shown in Fig. 11 and Fig. 9. (A) 1000 m long dike. (B) 5000 m long dike.



through the anomaly is shown in Figure 12B. The P-P amplitude is 90 nT whereas the induction-only anomaly in Figure 2a has only a 28 nT P-P anomaly. Although remanence makes for a more ambiguous interpretation, the increased size of the anomaly makes it more easily detectable.

#### 4.2 North-south oriented dikes

As shown by Beard (2000), for north-south striking dikes, a wide variety of remanence directions result in an anomaly pattern in which the anomalies at the terminal points of the dike appear to have been rotated. However, as in the previous example, a steeply inclined remanent direction  $180^\circ$  opposite the ambient field direction can produce an anomaly pattern similar to that of the buried cubic body. Shown in Figure 13a is the plan view anomaly of a dike identical in all respects to that of Figure 11, except that it possesses remanent magnetization. The Q-value is 2 and the remanent direction is  $180^\circ$  (directly opposite the ambient field) and at an inclination of  $70^\circ$ . The anomaly has two lobes of opposite polarity and both lobes have approximately the same magnitude—17 nT. If the dike is longer, 5000 m instead of 1000 m, the same remanent magnetization causes a separate and distinct 17 nT negative lobe at the north end of the dike and an identical positive lobe at the south end, as shown in Figure 13B.

### 5 FILTERS

The filtering of low latitude magnetic data is a controversial subject, and one fraught with difficulties. The reduction-to-pole (RTP) filter—commonly applied to middle- and high latitude data is unstable at equatorial latitudes and introduces artifacts in the form of north-south trending distortions. Considerable research has gone into this problem. Silva (1986) developed an equivalent source technique that reduces instabilities, but comes at the expense of considerably more computational expense. Hansen and Pawlowski (1989) report significant improvement using Weiner filtering. However, both papers show theoretical results based on equidimensional prism models, leaving open the question of how well their methods would behave under the more extreme signal-to-noise conditions found when elongate structures trend nearly north-south.

In contrast to the RTP filter, the reduction-to-equator (RTE) filter is quite stable irrespective of latitude. The advantage of an RTE filter is that it centers anomalies over their respective sources, much as does the RTP filter. However, the anomalies tend to be stretched in the east-west direction, and in the view of some workers, RTE filtering makes a bad situation even worse (Pearson, 1998). In my opinion, if the geophysical interpreter is sufficiently familiar with equatorial latitude magnetic data, RTE filtering can be used advantageously.

Analytic signal computations seem to be useful in enhancing low latitude anomalies (Qin, 1994). The analytic signal approach also appears to have advantages over the RTP filter when remanent magnetization is significant (Beard, 2000).

## 6 FIELD EXAMPLES—ETHIOPIA AND ERITREA

In this section, we illustrate some problems encountered in real data using data collected in Ethiopia and Eritrea.

Shown in Figure 14A is the magnetic total field anomaly from a portion of an airborne survey carried out in Ethiopia. The survey location lies between 2° and 6° north of the magnetic equator. In detail the greenstone belt geology of the area is quite complex, but for purposes of this discussion may be divided between a thick sequence of Tertiary basalts in the east, and an assortment of acid igneous intrusives, metasediments, and metavolcanics in the west and south. The north-south striking contact between the Tertiary volcanics and the other units strikes is a major geological feature. Radiometric data and electromagnetic data (not shown) clearly differentiate the basalts from the other units. The basalts probably have higher magnetic susceptibilities than most of the rock units to the west, much of which is composed of marble, yet because of the north-south strike of the contact, the unit is virtually invisible on the total magnetic field data. The total field anomaly map shows a distinct east-west trend, in spite of the general north-south strike of units in the area. This pattern can be deceptive, but is commonly seen in equatorial magnetic data, irrespective of structural strike.

Figures 14B and 14C show how the analytic signal and derivative maps can be advantageous in interpreting equatorial data. The analytic signal is a combination of the horizontal and vertical gradients of an anomaly. In Figure 14B, a 3-D analytic signal (Roest, et al., 1992) was computed from the total field data shown in Figure 14A. Susceptibility differences in the basalts result in gradients within the unit that are larger than in the metasediments. This results in an enhancement of the analytic signal over the basalts that differentiates them from the lower gradient metasediments. For the same reason, the second vertical derivative of the total field shows greater variation over the basalts, separating them from the metasediments.

Figure 14D shows the map resulting from application of a reduce-to-pole filter to the total field data. In this section of the surveyed area, the RTP filter does not appear to produce extreme north-south distortion. In other parts of the survey area the distortion is clear. To reduce north-south distortion it was necessary to apply a correction in order to keep the stabilize amplitude term in the RTP transformation (Geosoft, 1990). Unfortunately, this has the effect of reducing the amplitudes of the transformed anomalies, thus making it difficult to accurately model the RTP transformed field or perform Euler depth estimates. Nonetheless, in this case the RTP filtered results make clearer the locations of a few discrete bodies and

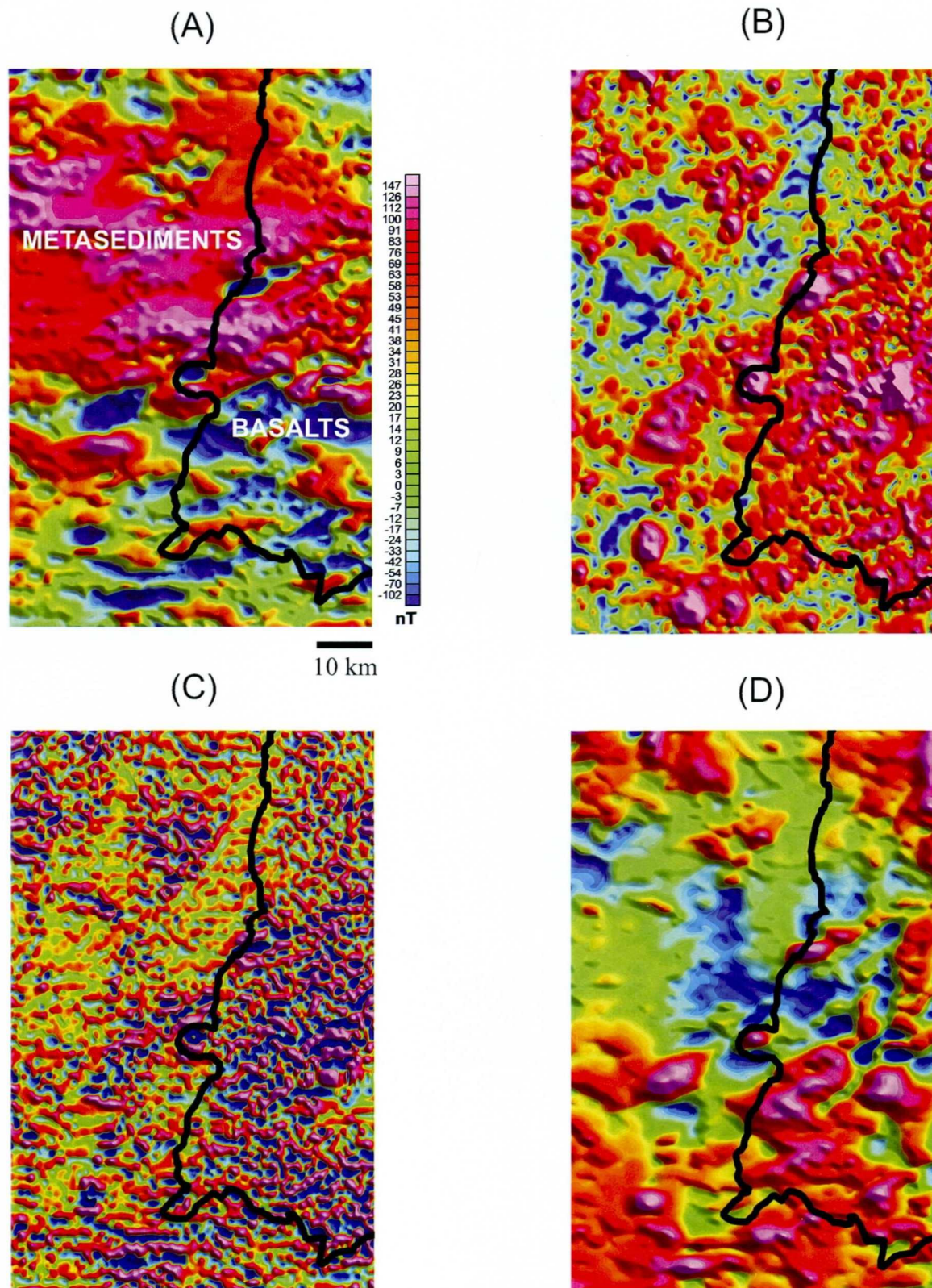


Fig. 14. Aeromagnetic data collected near the magnetic equator, Africa. (A) Total magnetic field upward continued to a height of 400 m above ground level. (B) Analytic signal of the total magnetic field. (C) Second vertical derivative of total field. (D) Total field reduced to pole.

faults that are not as immediately apparent in Figure 14A, although it fails to image the basalt-metasediment contact.

Figure 15A shows total field aeromagnetic data from western Eritrea. The magnetic latitude of the area shown is about  $14^{\circ}\text{N}$ . Magnetic declination is about  $1.5^{\circ}$  east of north. Geological mapping has thus far failed to reveal the source of the prominent anomaly in the center of the figure. A north-south profile across the anomaly is shown in Figure 15B. If we assume induction effects dominate remanence, then the profile can be modeled by either an equidimensional prism (see Fig. 2) or by a north-south trending elongate body dipping to the north. In this case, geological considerations, such as a dominant NE-SW strike, make the equidimensional body seem to be the more likely choice. Gravity data could be useful in resolving the ambiguity.

## 7 DISCUSSION AND CONCLUSIONS

At high latitudes, magnetic anomalies may closely mimic the shape of their source structures. A casual look at a high latitude aeromagnetic map is usually sufficient to identify the presence of major magnetic structures and the general structural strike of the area. To do the same with low latitude data requires much more experience. Low latitude magnetic anomalies tend to spread out in an east-west direction and end abruptly in the north and south directions. North-south trending structures may be magnetically invisible. This causes the anomaly patterns to have an east-west trend, regardless of the structural strike. The interpreter used to high latitude magnetic maps may reckon the structural strike to be more east-west than it actually is. The temptation can be hard to resist. Unavoidably, more work and more careful consideration of low latitude data is required to get reliable information than is the case with high latitude data. Various filters may be applied to enhance interpretation, but in my opinion the interpreter must carefully consider the total field data in light of known geological information, including existing rock properties data, before relying on filters.

If geological structures have a north-south trend, they may be very difficult to discern in the magnetic data. If such a magnetic body is sufficiently near the surface, its north and south terminations may be evident as positive-negative anomaly pairs. The positive lobe will lie mostly outside the extreme north or south edge of the body, and the negative lobe will lie over the body. Thus, if there is reason to expect a long, dipping structure striking north-south, it is possible to assess the direction of dip from a single termination anomaly. Furthermore, the positive lobe will have roughly the same magnitude as the negative lobe. This pattern may also occur in compact, equidimensional bodies, but only if remanent magnetism is dominant and the direction is opposite the inducing field, and at a steep inclination. Compact bodies in which induced magnetization is dominant will have negative lobes of considerably greater amplitude than their adjacent positive lobes.

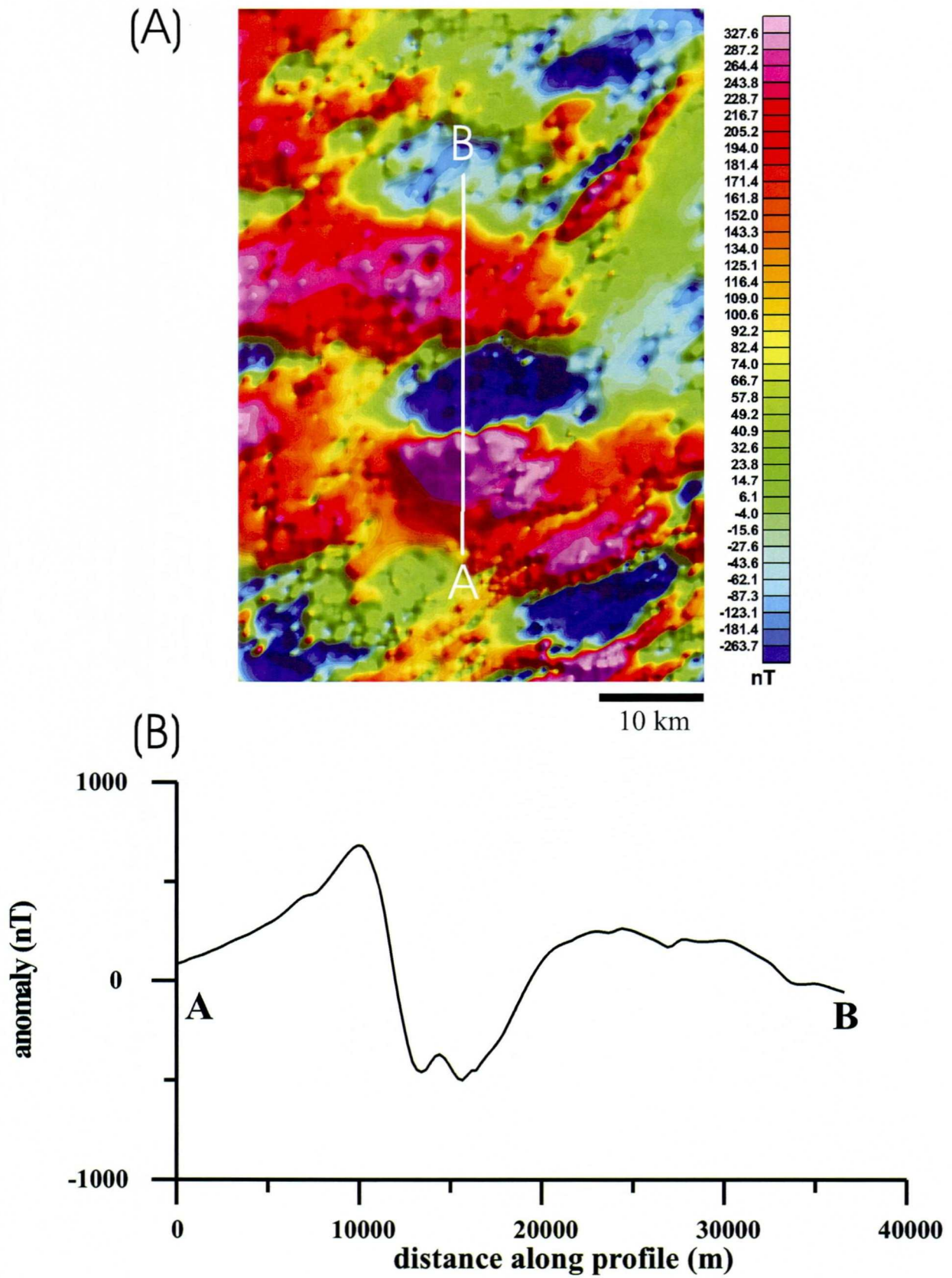


Fig. 15. Aeromagnetic data, western Eritrea. (A) Plan view and (B) profile of anomaly.

## 8 ACKNOWLEDGMENTS

NGU Project 2818.00-'Improved interpretation of low latitude magnetic anomalies'—was sponsored entirely by the Geological Survey of Norway. We thank the Geological Survey of Ethiopia and the Eritrean Geological Survey for permission to use aeromagnetic data shown in this report.

## 9 REFERENCES

Beard, L.P. 1998: Data acquisition and processing—helicopter geophysical survey, Oppkuven and Gran, 1997: NGU Report 98.079.

Beard, L.P., 1999: Detection of north-south trending magnetic structures at low latitudes: Proceedings of 61<sup>st</sup> EAGE Conference, Helsinki (Extended abstract).

Beard, L.P., 2000: Detection and identification of north-south trending magnetic structures near the magnetic equator: *Geophysical Prospecting*, 48, 745-761.

Beard, L.P. and Goitom, B., 2000: Some problems in interpreting low latitude magnetic surveys: Proceedings of the 6<sup>th</sup> Meeting of the Environmental and Engineering Geophysics Society, Bochum (Extended abstract).

Blakely, R.J., 1995: *Potential theory in gravity and magnetic applications*: Cambridge University Press, New York, 441 pp.

Clark, D.A., 1994: Magnetic petrophysics and magnetic petrology: aids to geological interpretation of magnetic surveys: *AGSO Journal of Australian Geology and Geophysics*, 17, 83-103.

Drew, G.J. and Cowan, D.R., 1994: Geophysical signature of the Argyle lamproite pipe, 393-402 in *Western Australia in Geophysical Signatures of Western Australian Mineral Deposits* (Eds: M.C. Dentith, K.F. Frankcombe, S.E. Ho, J.M. Shepherd, D.I. Groves, and A. Trench), University of West Australia Publication No. 26.

Eskola, L., Puranen, R., and Soininen, H., 1999: Measurement of magnetic properties of steel sheets: *Geophysical Prospecting* 47, 593-602.

Geosoft, 1996: *MAGMAP User Guide, 2-D frequency domain processing of potential field data*: Geosoft, Inc., Toronto, 54 pp.

Hansen, R.O. and Pawlowski, R.S., 1989: Reduction to pole at low latitudes by Wiener filtering: *Geophysics* 54, 1607-1613.

Pearson, W.C., 1998: Magnetic reduction-to-the-pole at low latitudes in *Geological Applications of Gravity and Magnetism: Case Histories* (eds: R. Gibson and P. Milligan): SEG Geophysical Reference Series No. 8 SEG, Tulsa, OK.

Qin, S., 1994: An analytic signal approach to the interpretation of total field magnetic anomalies: *Geophysical Prospecting* 42, 665-676.

Ravat, D., 1996: Magnetic properties of unruled steel drums from laboratory and field-magnetic measurements: *Geophysics* 61, 1325-1335.

Roest, W., Verhoef, J., and Pilkington, M., 1995: Magnetic interpretation using the 3-D analytic signal: *Geophysics* 57, 116-125.

Silva, B.C.J., 1986: Reduction to the pole as an inverse problem and its application to low latitudes: *Geophysics* 51, 369-382.

Telford, W.M., Geldart, L.P., and Sheriff, R.E., 1993: *Applied Geophysics*, 2<sup>nd</sup> Ed. Cambridge University Press, New York, 770 pp.

Thorpe, R. and Brown, G., 1985: *The Field Description of Igneous Rocks*, Open University Press, Buckingham, England, 155 pp.